Growth Rates of Phosphate Nodules from the Continental Margin Off Peru

Abstract. *Modern sea-floor phosphorite nodules sampled from off the coast of Peru are shown to grow at rates of millimeters per thousand years in spite of the fact that the measured accumulation rates of the underlying sediment are two to four orders of magnitude faster. Phosphate nodules grow downward into soft sediment, and the rates of phosphorus accumulation into nodules are approximately equal to the upward diffusive flux of dissolved phosphate inferred from pore water profiles. These results demonstrate that phosphorus in nodules originates from regeneration in sediments rather than as a result of direct precipitation from bottom waters.*

Phosphate deposits of the sea floor are particularly common in regions of coastal upwelling. Most ocean floor deposits are relict although modern formation has been identified at a few sites, primarily in areas of intense coastal upwelling, for example, off Peru and Namibia (*1*). The phosphate nodules of the Peru-Chile continental margin range in age from Holocene to late Pleistocene, occur at the sediment-water interface, and apparently form preferentially near the upper and lower boundaries of the intersection of the oxygen minimum zone with the continental margin (*2*). Earlier determinations of the uranium-series ages of these phosphate nodules have been based on bulk analyses of homogenized powders. We report here the first attempts to determine the growth rates of marine phosphorite nodules by uranium disequilibrium dating of discrete sections through individual nodules. A knowledge of the growth rates of phosphate nodules is considered critical both to our understanding of the genesis of these deposits and to an assessment of the importance of phosphorites in the marine geochemical cycle of phosphorus (*3*). Furthermore, our results for Peruvian phosphorites may be useful as an analog for ancient deposits such as the phosphatic sections of the Monterey Formation (California), reported to contain phosphate nodules in a silica-rich matrix (*4*).

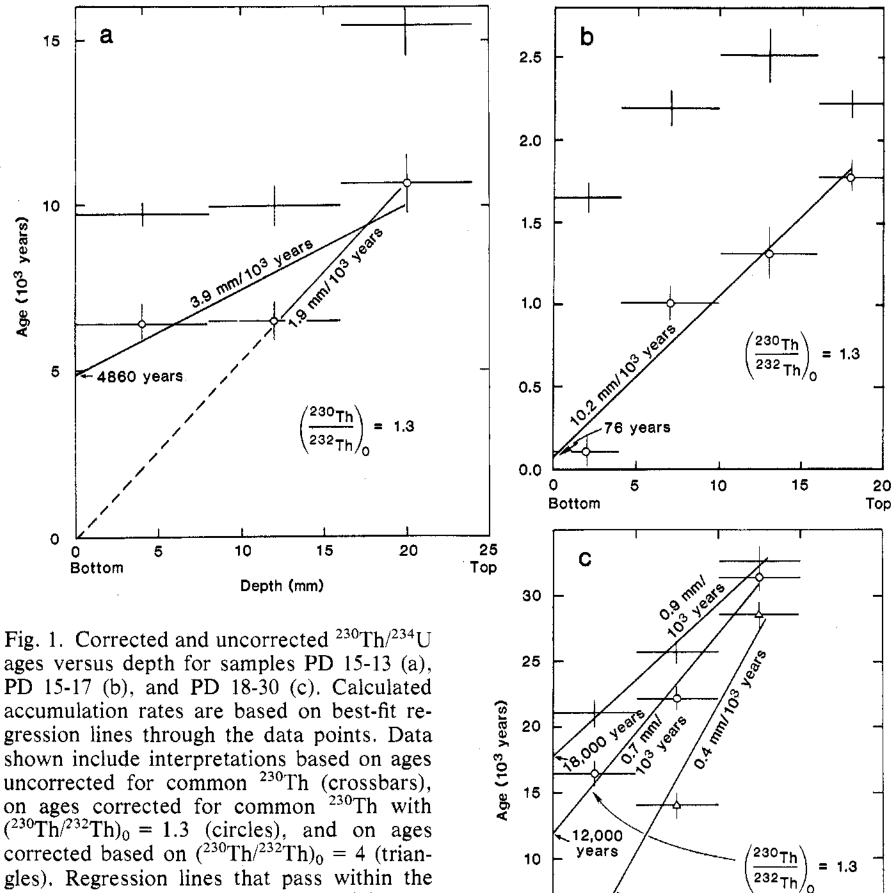

Fig. 1. Corrected and uncorrected ^{230}Th/^{234}U ages versus depth for samples PD 15-13 (a), PD 15-17 (b), and PD 18-30 (c). Calculated accumulation rates are based on best-fit regression lines through the data points. Data shown include interpretations based on ages uncorrected for common ^{230}Th (crossbars), on ages corrected for common ^{230}Th with (^{230}Th/^{232}Th)$_0$ = 1.3 (circles), and on ages corrected based on (^{230}Th/^{232}Th)$_0$ = 4 (triangles). Regression lines that pass within the analytical uncertainty through the origin may indicate that a nodule was actively growing when sampled. Positive intercepts on our uranium-series age axis indicate that active growth ceased at that time.

Three samples were selected for our study that were (i) young, providing a higher probability of measuring a gradient in radiogenic ^{230}Th; (ii) relatively flat, so that it was possible to cut a series of contiguous slices a few millimeters thick through each nodule; and (iii) capable of being oriented with respect to top and bottom on the basis of an oxidized layer on the exposed surface. Each nodule was sectioned into three or four slices perpendicular to the suspected growth axis and then powdered, dried, radiochemically separated, and analyzed for uranium-series isotopes by standard techniques (*2*).

The results of the radiochemical analyses are presented in Table 1 (*5*). In order to calculate meaningful absolute ages from the uranium-series results, it is necessary to correct for common ^{230}Th present in the nodule not as a result of radioactive decay from its parent uranium but in association with ^{232}Th contamination. If we assume that nonradiogenic thorium is incorporated into the nodules early in their history with a fixed ^{230}Th/^{232}Th activity ratio, we can correct for the presence of this common ^{230}Th by the method of Kaufman and Broecker (*6*).

The value assigned to the initial ^{230}Th/^{232}Th activity ratio [(^{230}Th/^{232}Th)$_0$] is somewhat uncertain. Burnett and his co-workers suggested a value of 4 (*2*) on the basis of measurements of very young phosphate samples and Recent associated sediment from the Peru shelf. Twc out of the three samples reported here have measured ^{230}Th/^{232}Th activity ratios lower than this value; these results imply that (^{230}Th/^{232}Th)$_0$ is lower in these cases. The lower ^{230}Th/^{232}Th activity ratios measured in these samples may be due to differences in sample preparation (*7*). Since the ^{232}Th is considered to be associated with the impurities in these samples (*8*), the value of unity for the ^{230}Th/^{232}Th activity ratio for average river sediment reported by Scott (*9*) may also serve as a useful guide for an initial value. Measurements of the isotopic composition of thorium in the acid-soluble fractions of Recent sediments from the upwelling zone off Baja California, Mexico, gave a range of ^{230}Th/^{232}Th activity ratios from 1.4 to 1.7 in nine determinations (*10*). These data lead us to conclude that the value of (^{230}Th/^{232}Th)$_0$ in these samples lies between 1 and 1.4,

Table 1. Radiochemical results from slices of nodules PD 15-13, PD 15-17, and PD 18-30, from off the coast of Peru. All ratios are activity ratios, and errors shown are ± 1σ, based on counting statistics. Ages are calculated both on the basis of corrected and uncorrected $^{230}Th/^{234}U$ activity ratios; ppm, parts per million.

Layer (mm)	U (ppm)	Th (ppm)	$^{230}Th/^{232}Th$	$^{234}U/^{238}U$	$^{230}Th/^{234}U$	$^{230}Th_c/^{234}U$*	Ages (10^3 years)	
							Uncorrected	Corrected
Sample PD 15-13 (15°13.3'S, 75°22.2'W; 120 m)								
0 to 8	46.4	3.61	3.8 ± 0.3	1.16 ± 0.02	0.086 ± 0.003	0.058	9.8 ± 0.4	6.5
8 to 16	30.8	2.67	3.6 ± 0.4	1.18 ± 0.02	0.088 ± 0.005	0.059	10.0 ± 0.6	6.6
16 to 24	23.5	2.65	4.0 ± 0.3	1.12 ± 0.02	0.133 ± 0.006	0.094	15.5 ± 0.8	10.7
Sample PD 15-17 (15°17.8'S, 75°23.5'W; 370 m)								
0 to 4	119	4.40	1.4 ± 0.1	1.14 ± 0.01	0.0151 ± 0.0008	0.0010	1.65 ± 0.09	0.1
4 to 10	125	3.53	2.4 ± 0.2	1.15 ± 0.01	0.020 ± 0.001	0.0093	2.2 ± 0.1	1.0
10 to 16	92.6	2.77	2.7 ± 0.3	1.16 ± 0.02	0.023 ± 0.001	0.0120	2.5 ± 0.2	1.3
16 to 20	187	2.01	6.5 ± 0.6	1.14 ± 0.01	0.0203 ± 0.0008	0.0163	2.23 ± 0.08	1.8
Sample PD 18-30 (18°30.0'S, 70°36.5'W; 385 m)								
0 to 5	23.2	2.70	5.4 ± 0.4	1.18 ± 0.02	0.177 ± 0.007	0.140 (0.052)†	21.1 ± 1.0	16.4 (5.8)
5 to 10	29.4	2.55	8.3 ± 0.5	1.14 ± 0.01	0.211 ± 0.006	0.184 (0.121)	25.7 ± 0.8	22.1 (14.0)
10 to 15	84.6	2.49	30 ± 2	1.14 ± 0.01	0.260 ± 0.007	0.251 (0.232)	32.7 ± 1.0	31.4 (28.6)

*$^{230}Th_c = {}^{230}Th_m - (^{230}Th/^{232}Th)_0 \times {}^{232}Th\ e^{-\lambda t}$, where $^{230}Th_m$ is the measured value, λ is the decay constant of ^{230}Th (9.22×10^{-6} year^{-1}), and t is time; $(^{230}Th/^{232}Th)_0 = 1.3$. †Values in parentheses are calculated for $(^{230}Th/^{232}Th)_0 = 4$.

Table 2. Accumulation rates of phosphorus in three phosphate nodules from off the coast of Peru. Growth rates are from the age-depth curves (Fig. 1). Bulk densities for all three samples (2.4 g cm^{-3}) are based on the average of six measurements of sample PD 18-30.

Sample	Phosphorus (10^3 μmole g^{-1})	Growth rate (mm per 10^3 years)	Phosphorus accumulation rates (10^{-9} μmole cm^{-2} sec^{-1})
PD 15-13	2.25	4	68
PD 15-13	2.25	2	34
PD 15-17	2.77	10	210
PD 18-30	2.94	1	22
PD 18-30	2.94	0.4	9

the lowest value measured in our samples. We therefore adopted an initial value of 1.3 for $(^{230}Th/^{232}Th)_0$ to calculate ages for all nodules. It is very possible that $(^{230}Th/^{232}Th)_0$ varies from nodule to nodule. A higher value (of 4) was also used in the case of sample PD 18-30. The value of 1.3 produced the best fit of the corrected data in sample PD 15-17, the youngest and most densely analyzed sample.

We have plotted both corrected and uncorrected uranium-series ages versus depth measured from the bottom surfaces in order to assess the growth rates of these nodules (Fig. 1). The results suggest that these phosphate nodules grow slowly, on the order of < 1 to 10 mm per thousand years. This slow growth rate is surprising in view of the rapid sedimentation rates reported for this area (millimeters to centimeters per year) (*11*). Peru phosphate nodules grow at roughly uniform rates for periods of thousands of years. Sample PD 15-13 may be an exception, with slow initial growth followed by very rapid growth. Because this interpretation relies heavily on a single data point, we prefer to use a best-fit line to derive a growth rate for this sample. Thus, these nodules remain at the sediment-water interface for periods surprisingly long as compared to the rates of associated sediment accumulation. Even our fastest-growing nodule, sample PD 15-17, took almost 2000 years to form. At a rate of sediment accumulation of approximately 1 mm per year, sample PD 15-17 should have been buried under about 2 m of sediment!

Our age-depth curves also show that, unlike manganese nodules which grow in all directions, these nodules grow down (the tops are oldest) into the sediment. This observation, together with our growth rate data, suggests that the source of phosphorus and other elements contained within these nodules is sediment interstitial waters. The accumulation rates of phosphorus in these nodules, based on our measurements of growth rates, phosphorus concentrations, and bulk densities, range from about 10×10^{-9} to 200×10^{-9} μmole cm^{-2} sec^{-1} (Table 2), reflecting differences in the measured growth rates. Suess (*12*) calculated an average diffusive phosphate flux from the sediments into bottom waters of 65×10^{-9} μmole cm^{-2} sec^{-1}; his value was based on pore water profiles of dissolved phosphate in five cores from the Peru upwelling zone. This flux is more than sufficient to supply phosphate to two of the three nodules examined, although low but still of the same magnitude required for the fastest growing nodule, sample PD 15-17. We believe that these determinations are sufficiently close to suggest that the upward diffusive flux of phosphate to the sediment-water interface on the Peru shelf is sufficient to supply the phosphorus contained in these nodules. In addition to phosphorus, the relatively high $^{234}U/^{238}U$ activity ratios measured in these samples may also suggest uranium supply from pore solutions rather than seawater, as the soluble uranium of anoxic pore waters has a higher $^{234}U/^{238}U$ activity ratio than seawater (*13*).

WILLIAM C. BURNETT
MICHAEL J. BEERS
KEVIN K. ROE

Department of Oceanography,
Florida State University,
Tallahassee 32306

References and Notes

1. Y. Kolodny and I. R. Kaplan, *Geochim. Cosmochim. Acta* **34**, 3 (1970); G. N. Baturin, K. I. Merkulova, P. I. Chalov, *Mar. Geol.* **13**, M37 (1972); H. H. Veeh, W. C. Burnett, A. Soutar, *Science* **181**, 844 (1973); A. G. Kress and H. H. Veeh, *Mar. Geol.* **36**, 143 (1980); G. W. O'Brien and H. H. Veeh, *Nature (London)* **288**, 690 (1980).
2. W. C. Burnett and H. H. Veeh, *Geochim. Cosmochim. Acta* **41**, 755 (1977); ———, A. Soutar, *Soc. Econ. Paleontol. Mineral. Spec. Publ. 29* (1980), p. 61.
3. P. N. Froelich, M. L. Bender, N. A. Luedtke, G. R. Heath, T. J. DeVries, *Am. J. Sci.*, in press.
4. K. A. Pisciotto, thesis, University of California, Santa Cruz (1978).
5. Our results are in satisfactory agreement with those published earlier (*2*), except for nodule PD 18-30 which was older (higher $^{230}Th/^{234}U$) than expected. This does not imply a discrepancy, however, as these samples are not true replicates but different nodules recovered from the same dredge haul. Thus, samples from nearly the same site do not necessarily have the same uranium-series age.
6. A. Kaufman and W. Broecker, *J. Geophys. Res.* **70**, 4039 (1965).
7. In our earlier measurements we used a total

dissolution technique. The results reported here are based on the acid-soluble fraction.
8. These samples are known to contain varying quantities of quartz, feldspar, clay minerals, and biogenic materials as well as carbonate fluorapatite [W. C. Burnett, *Geol. Soc. Am. Bull.* **88**, 813 (1977)].
9. M. R. Scott, *Earth Planet. Sci. Lett.* **4**, 245 (1968).
10. R. Jahnke, S. Emerson, K. K. Roe, W. C. Burnett, in preparation.
11. D. J. DeMaster, thesis, Yale University (1979); S. M. Henrichs, thesis, Woods Hole Oceanographic Institution (1980).
12. E. Suess, *Geochim. Cosmochim. Acta* **45**, 577 (1981).
13. J. K. Cochran and S. Krishnaswami, *Am. J. Sci.* **280**, 849 (1980).
14. The constructive criticisms of an earlier draft of this report by P. N. Froelich, D. Z. Piper, and J. K. Osmond are gratefully acknowledged. We thank A. Soutar for supplying samples. The research reported here was supported by NSF grant OCE-8007047 to W.C.B. This report is a contribution to Project 156 (Phosphorites) of the International Geological Correlation Program.

21 July 1981; revised 3 December 1981

Coral Gas: Oxygen Production in *Millepora* on the Great Barrier Reef

Abstract. *Large volumes of a gas consisting of 69 percent molecular oxygen and 31 percent molecular nitrogen with trace amounts of carbon monoxide, carbon dioxide, and methane have been found trapped inside skeletons of the common hydrozoan* Millepora. *Volumes were low in the morning and reached a maximum by late afternoon. The oxygen was probably produced by the endolithic (boring) algae, with which the* Millepora *skeletons are very heavily infested. Oxygen production by endolithic algae in* Millepora *and in other substrates could influence estimates of reef productivity based on measurements of dissolved gases.*

Concentrations of dissolved gases in reef waters have been used for some time to estimate rates of calcification, respiration, and photosynthesis (*1*, *2*). In some of these studies (*2*), it has been suggested that "skeletal algae" (in fact, endolithic or boring algae) may play a major role in O_2 production, but most recent studies have tended to ignore the endoliths completely (*3*). Recent observations on the Great Barrier Reef of gas trapped inside skeletons of the common hydrozoan *Millepora* (stinging or fire coral) suggest that large amounts of O_2 can be produced by endolithic algae in reef ecosystems.

During scuba diving associated with general research on bioerosion in the central region of the Great Barrier Reef, we incidentally observed gas bubbling from freshly broken branches of several species of *Millepora*. Further observations showed that, although the volumes of trapped gas were very low or undetectable in early morning, by late afternoon a freshly broken branch of *Millepora* could exude a fine stream of bubbles for up to half a minute (Fig. 1A). The gas is under such pressure that it will bubble down and out of a broken-off branch held vertically. One of us (M.J.R.) insists that he heard the hiss of escaping gas on several occasions when a piece of coral was broken. The gas has been found in *Millepora* at all depths between −1 and −20 m.

Samples collected for analysis (*4*) showed the gas to be, by volume, 69.3 percent O_2, standard deviation = 8.0, and 30.7 percent N_2, standard deviation = 3.5 (N = 15), with traces (< 0.1 percent) of CO, CO_2, and CH_4. Although O_2 is produced by symbiotic algae (zooxanthellae) associated with coelenterate hosts (*5*), this process is unlikely to be the source of the O_2 described here. The

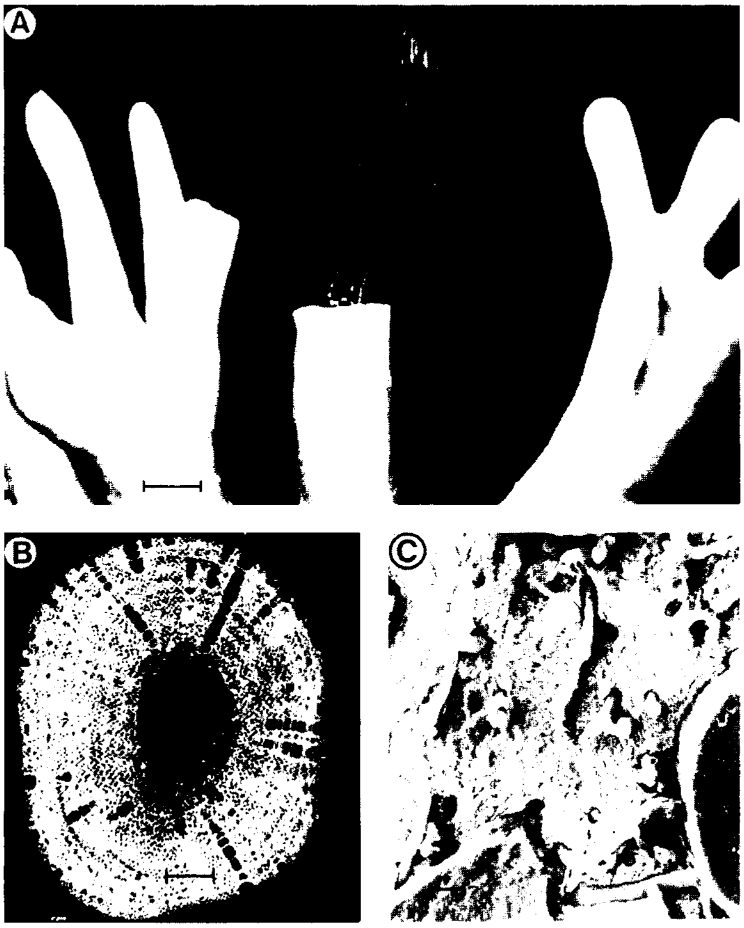

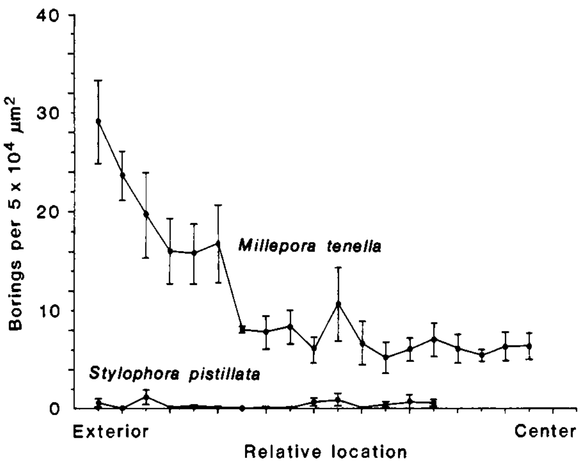

Fig. 1 (left). (A) Gas escaping from a freshly broken branch of *Millepora tenella*: sample from −10 m, Britomart Reef. Scale bar, 5 mm. (B) Thin section of *Millepora tenella* skeleton showing the porous coenosteum, corallites (dactylopores and gastropores) with complete tabulae, and the highly porous central region. Scale bar, 1 mm. (C) Scanning electron micrograph of borings in *Millepora tenella* (coenosteum: Spurr impregnation, weak acid etch). Scale bar, 20 μm. Fig. 2 (right). Relative intensity of algal borings in *Millepora tenella* and *Stylophora pistillata* (a scleractinian coral with a branching habit similar to that of *Millepora*). Samples were from −10 m, Britomart Reef. The bars represent the range of at least five measurements in all cases, from several different coral samples.